Geophysical Research Letters

RESEARCH LETTER
10.1029/2024GL111069

Wave-Influenced Delta Morphodynamics, Long-Term Sediment Bypass and Trapping Controlled by Relative Magnitudes of Riverine and Wave-Driven Sediment Transport

F. Zăinescu[1,2], J. E. A. Storms[3], A. Vespremeanu-Stroe[2], H. Van Der Vegt[4], M. Schuster[5], and E. Anthony[1]

[1]AMU, CNRS, IRD, INRAE, Coll France, CEREGE, Aix-en-Provence, France, [2]Faculty of Geography, UniBuc, Bucharest, Romania, [3]Faculty of Civil Engineering and Geosciences, Delft University of Technology, Delft, The Netherlands, [4]Deltares, Delft, The Netherlands, [5]CNRS, UNISTRA, ITES, UMR 7063, Strasbourg, France

Abstract River sediment supply (*Qs*) and longshore sediment transport (*LST*) are recognized as two paramount controls on river delta morphodynamics and stratigraphy. We employed the Delft3D model to simulate the evolution of deltas from fluvial to wave-dominated conditions, revealing the interplay between river- and wave-driven sediment quantities. Wave-influenced deltas may show alternating accumulation and retreat patterns driven by avulsions and wave-induced sediment diffusion, posing coastal management challenges. Deltas with higher wave energy evolve under a fine balance between river supply and intense wave-mediated sediment redistribution and are highly vulnerable under conditions of sediment reduction. Reducing *Qs* by ~40%–70%, common in modern dammed rivers, can rapidly shift bypass from ~0 to 1 (no bypass to complete bypass). This leads to accelerated diffusion and potential sediment loss in modern deltas. The study highlights the importance of accurately computing sediment quantities in real-world deltas for improved management, especially under increasing anthropogenic and climatic pressures.

Plain Language Summary Ocean waves, like proficient sculptors, shape the meeting points of rivers and seas—where deltas are created. Under the power of ocean waves, the sediments transported by rivers are organized into distinct patterns. Using an advanced computer model, our research unveils how this interplay affects the physical form of these deltas and their functioning. In certain conditions, the sediment carried by waves can jump over the river mouth and move further along the coastline, contributing to stretching the delta and inducing erosion. Currently, river sediments are getting blocked behind river dams, depriving deltas of their sediment nourishment. As sediment supply decreases, powerful waves at the sea erode deltas more easily, endangering ecosystems, human communities and infrastructure. Because deltas are facing challenges from climate change and increased human activities, informed and innovative management strategies based on better knowledge of natural processes are needed to preserve these valuable coastal regions.

Key Points:

- Deltas transition from avulsion-dominated with localized depocenters to more diffuse and alongshore-deflected wave-dominated depocenters
- Bypass increases and trapping decreases abruptly when longshore transport (*LST*) at the river mouth equals river sediment transport (Q_s)
- *LST* under large-scale blocking due to mouth bar and shoreface adjustment feeds wave-dominated updrift beach ridge plains (strandplains)

Supporting Information:

Supporting Information may be found in the online version of this article.

Correspondence to:

F. Zăinescu,
zaiflorin@gmail.com

Citation:

Zăinescu, F., Storms, J. E. A., Vespremeanu-Stroe, A., Van Der Vegt, H., Schuster, M., & Anthony, E. (2024). Wave-influenced delta morphodynamics, long-term sediment bypass and trapping controlled by relative magnitudes of riverine and wave-driven sediment transport. *Geophysical Research Letters*, *51*, e2024GL111069. https://doi.org/10.1029/2024GL111069

Received 4 JUL 2024
Accepted 24 SEP 2024

Author Contributions:

Conceptualization: F. Zăinescu, E. Anthony
Data curation: F. Zăinescu
Formal analysis: F. Zăinescu
Funding acquisition: A. Vespremeanu-Stroe, M. Schuster
Methodology: F. Zăinescu, J. E. A. Storms, H. Van Der Vegt, E. Anthony
Project administration: A. Vespremeanu-Stroe, M. Schuster
Resources: M. Schuster
Software: F. Zăinescu, J. E. A. Storms, H. Van Der Vegt, M. Schuster

1. Introduction

Delta plain size scales with the magnitude of river sediment discharge (Aadland & Helland-Hansen, 2019; Anthony, 2015; Syvitski & Saito, 2007; Wright & Coleman, 1973), whereas marine forces notably influence the coastline and the subaqueous domain (Hori et al., 2002; Jerolmack, 2009; Leonardi et al., 2013; Walsh & Nittrouer, 2009; Wright & Coleman, 1972; Zăinescu et al., 2019). Waves reroute riverine sediment to craft delta lobes that balance with the boundary conditions (George & Hill, 2008; Nardin & Fagherazzi, 2012; Zăinescu, Storms, van der Vegt, et al., 2023), resulting in construction of beach-ridge plains, barriers and elongated spits that are an integral part of many deltas (Anthony & Blivi, 1999; Vespremeanu-Stroe et al., 2016).

In asymmetric wave-influenced deltas, waves arriving at an angle induce unidirectional longshore sediment transport (*LST*) at the coast. Sands, whether allochthonous or eroding from delta fronts, contribute to delta plain formation when trapped updrift of the river mouth whereas riverine fines predominantly accumulate downdrift creating stratigraphic asymmetry (Bhattacharya & Giosan, 2003; Khan et al., 2021; Preoteasa et al., 2016). Disparities in the growth rates on either side of the river mouth are often present (Korus & Fielding, 2015; Vespremeanu-Stroe et al., 2017), which can be enhanced by avulsions.

10.1029/2024GL111069

Supervision: E. Anthony
Validation: F. Zăinescu
Visualization: F. Zăinescu
Writing – original draft: F. Zăinescu
Writing – review & editing: F. Zăinescu, J. E. A. Storms, A. Vespremeanu-Stroe, E. Anthony

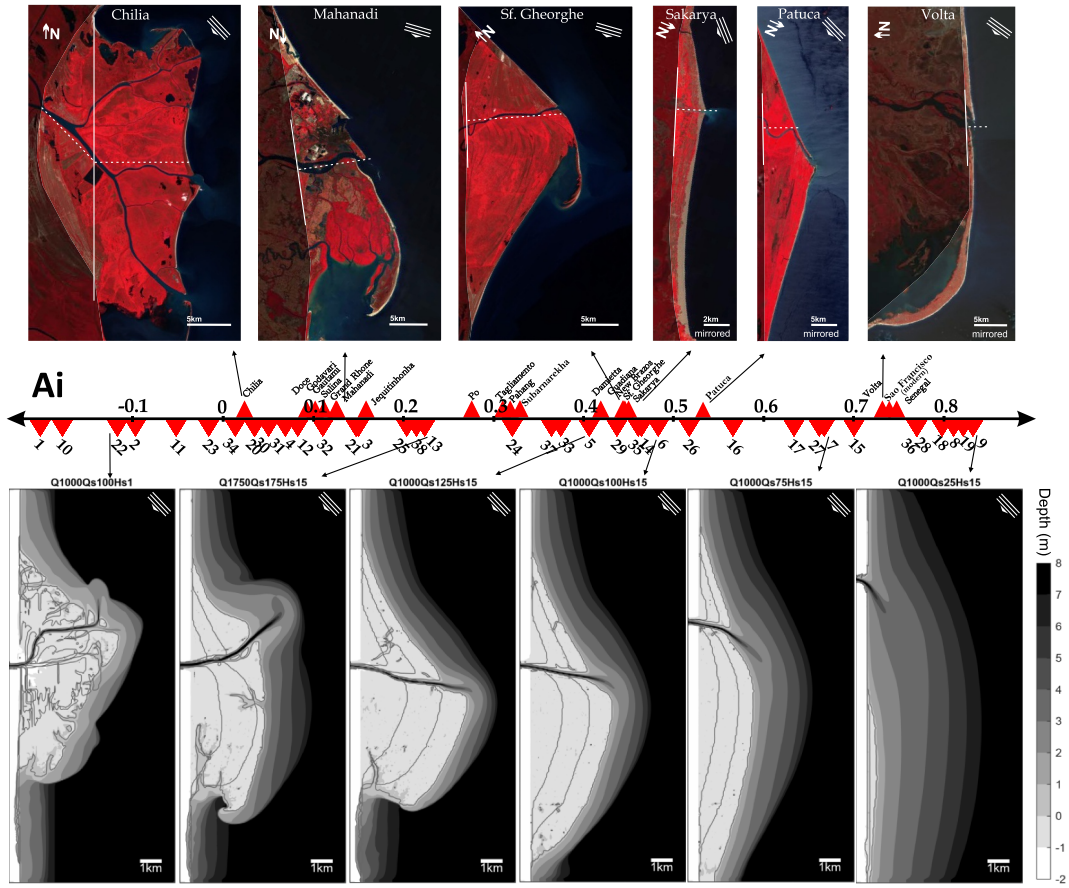

Figure 1. Asymmetry in wave-influenced deltas. Real-world examples (top) versus numerical results (bottom) aligned using the Asymmetry index (*Ai*). Increased *Ai* signifies more sediment redistribution downdrift and reduced sediment trapping near the river mouth. Gray contour lines show 1/3 and 2/3 of delta evolution. Simulation parameters in subplot titles are self-explanatory (see Table S1 in Supporting Information S1). Real-world examples are detailed in Table S2 in Supporting Information S1. Top: Sentinel 2 false composites from www.sentinel-hub.com. Limits for shaded areas are delineated from ridges or contact with mainland or from literature-based paleoreconstructions (Aagaard et al., 2021; Vespremeanu-Stroe et al., 2017). Central line determination (dotted white line). Primary wave direction is indicated with three parallel lines.

Balances in river and wave sediment fluxes are widely recognized as a determining factor in the morphodynamics of wave-influenced deltas. However, the determination of specific threshold values demarcating this balance remains challenging (Broaddus et al., 2022; Nienhuis et al., 2015; Preoteasa et al., 2016; Ratliff et al., 2018; Sadio et al., 2017; Syvitski et al., 2022; Wright & Coleman, 1973; Zăinescu et al., 2019).

Reduced-complexity delta shoreline evolution models like the Coastal Evolution Model (CEM) have been used to study wave-influenced deltas. The CEM initially featured straight advancing river mouths (Ashton & Giosan, 2011) and later incorporated river mouth mobility (Nienhuis, Ashton, & Giosan, 2016) and sediment bypassing (Gao et al., 2020) based on synthesizing Delft3D results which allowed the derivation of parameterizations to better represent these processes. While providing insight into wave spreading and river mouth directional change, these models struggle to simulate plan-shape asymmetry at low fluvial sediment discharges (Korus & Fielding, 2015) (Figure 1a). When total bypass is assumed (Hu et al., 2022), the increase in wave climate asymmetry imposes greater delta plan-form asymmetry. Ratliff et al. (2018) found that in wave-dominated deltas, river mouth progradation is slower and the avulsion timescale larger, but this effect is less pronounced in antidiffusive wave climates. However, CEM-like models omit river mouth behavior, rely on parametrized sediment bypass, and use simplified bathymetry and wave refraction processes (Robinet et al., 2018).

Modeling with full physics-based models like Delft3D has enabled significant strides in understanding longer-term fluvial evolution in deltas (van der Vegt et al., 2020), and short-term wave effects involved in the evolution of mouth bars and sediment bypassing (Edmonds et al., 2021; Nardin et al., 2013; Nienhuis, Ashton, Nardin, et al., 2016). Recently, Broaddus et al. (2022) reported a novel approach using Delft3D to quantify the role of sediment fluxes on shaping first-order delta morphology for mixed influenced deltas. This paper presents a novel Delft3D application simulating long-term evolution of asymmetric wave-influenced delta lobes. We focus on delta-lobe scale and address impacts of variable river mouth sediment bypassing in asymmetric, strongly wave-dominated climates, exceeding those in Broaddus et al. (2022). Our model generates realistic morphologies, and allows us to extrapolate sediment bypass over the river mouth based on the balance between Qs and LST. Understanding the long-term evolution of river deltas is vital, particularly as they face growing erosion risks due to anthropogenic perturbations of sediment supply and water discharge. The findings of this study can inform the development of reliable predictions and management strategies for the sustainable use of these dynamic, biodiversity-rich and often densely populated coastal landforms.

2. Numerical Modeling and Experimental Design

We use Delft3D coupled with SWAN to simulate 38 synthetic delta lobes under varying wave influence. Delft3D (Lesser et al., 2004), a comprehensive modeling suite for simulating hydrodynamic and morphological processes, has been widely applied to deltaic systems (Attema, 2014; Geleynse et al., 2011; Nardin & Fagherazzi, 2012; Storms et al., 2007; Su et al., 2017). It incorporates sedimentary and hydrodynamic processes, enabling morphologic feedbacks under wave forcing and directly modeling river mouth interactions controlling long-term sediment blocking or bypassing, surpassing previous reduced-complexity approaches. See Supporting Information S1 for full model details.

Following the asymmetric delta conceptual model established by Bhattacharya and Giosan (2003); we propose a novel numerical investigation with a physics-based model on long-term deltaic lobe asymmetry (Figure S1 in Supporting Information S1). We guided our simulations by first pre-computing various degrees of wave influence based on the Sedimentary index (Si, Preoteasa et al., 2016).

$$Si = \frac{LST}{Qs} \tag{1}$$

where LST is the value for the longshore sediment transport (m^3/yr) and Qs is the value for the total river sediment discharge (m^3/yr). The Si can be calculated using values of updrift LST entering the model domain (LST_{Up}, m^3/yr); or by using the maximum longshore sediment transport which occurs at the river mouth (LST_{MaxRM}, m^3/yr), a quantity similar to the one proposed by Nienhuis et al. (2015). The Si becomes either Si_{Up} or Si_{Max} when using either LST values, Table S1 in Supporting Information S1. For real-world deltas, Si_{Max} was computed from the global predictions of Nienhuis et al. (2020). More details on the computation of LST_{MaxRM} quantities and limitations of the global predictions are found in Texts S2 and S3 in Supporting Information S1. Higher values of Si indicate increasing wave domination. Significant wave height (Hs) varies between 0 and 1.7 m, and directions from 22.5 to 67.5°. Most simulations employ a Hs of 1.5 m approaching from 45° relative to the initial shoreline. Modeled LST_{Up} values vary from 0.01×10^6 m^3/yr (Hs 0.5 m) to 0.5×10^6 m^3/yr (Hs 1.5 m) to 1.25×10^6 m^3/yr (Hs 1.7 m). Water discharge (Q) varies from 250 to 2,000 m^3/s with the most frequent condition set at 1,000 m^3/s. Qs is set from 12,5–500 kg/s (equivalent to 0.27 to 10.35×10^6 m^3/yr calculated in-model at the boundary, including bedload). Sensitivity analyses concerning wave non-stationarity on the simulated results are presented in Figure S2 in Supporting Information S1. With the exception of three simulations that have variable wave heights, all other conditions are stationary. Full information on boundary conditions is provided in Table S1 in Supporting Information S1.

All simulated deltas have the same total amount of river sediment delivered at the end of the simulation to enable comparison of final delta morphologies; therefore, the total run time of the simulations changes proportionally with the change in Qs to reflect multidecadal to multi-centennial timescales of evolution.

The current model set-up reproduces numerous processes and morphologies at delta-lobe scale such as avulsions and riverine dynamics (channel erosion/accumulation), levee formation, wave-dominated shoreface formation,

delta front morphology, river-mouth bar generation (both symmetric and asymmetric) (Figure S3 in Supporting Information S1).

3. Results and Discussions

3.1. Delta Asymmetry: Model Versus Real-World

Synthetic and real-world deltas are compared using the asymmetry index (A_i) of Korus and Fielding (2015). The A_i is a normalized difference index that indicates the impact of marine controls on the seaward advancement of the depocenter through deviations away from the delta center line (Korus & Fielding, 2015). Center line determination is from lobe apex (at the river start) to paleoshoreline midpoint at onset of major progradation (Korus & Fielding, 2015). Direction may change at the point where it meets the pre-delta shoreline, accounting for the fact that deltas may occupy asymmetric embayments.

$$A_i = \frac{(D - U)}{(D + U)} \tag{2}$$

where D and U represent downdrift and updrift values, respectively, obtained as surfaces for real-world deltas and volumes for modeled deltas. Ai ranges from 0 (symmetric) to 1 (maximum downdrift asymmetry), with negative values indicating predominantly updrift growth. As wave influence increases relative to river influence, delta morphology shifts from river-dominated featuring multiple river mouths, to increasingly wave-dominated showing increased asymmetry under oblique waves (Figure 1). Low to moderate Ai (0.1–0.5) delta lobes develop arcuate to cuspate morphologies with quasi-triangular shapes that are skewed downdrift, and proportionally more beach ridges in natural deltas are indicative of waves. Straight to slightly concave shorelines develop updrift, whereas convex shorelines form downdrift, due to the differential effects of wave-climate asymmetry on alongshore sediment transport efficiency (Hu et al., 2022). Moderate Ai cases show spits downdrift both in real-world and models. Asymmetric lobes display extensive beach-ridge plains updrift and beach ridges and spits interspersed with marsh plains downdrift. In strongly asymmetric deltas ($Ai > 0.7$) such as the Volta and Senegal deltas, little sediment is trapped updrift, indicating intense bypassing across the river mouth, and sediment trapped downdrift at an increasing distance from the river mouth (Anthony et al. (2016); Sadio et al. (2017)).

Depending on the value of Ai, simulated delta lobes became more or less protruding and asymmetric, mimicking variability found in natural morphologies (Figure 1). Synthetic deltas obtain higher asymmetry with increasing relative wave power with regards to Q_s, creating higher LST redistribution alongshore from the river mouth.

3.2. Long-Term Sediment Bypass and Total Delta Sediment Trapping

Long-term sediment bypassing (β) is the fraction of total wave-derived updrift longshore sediment transport (LST_{Up}) that enters the domain and crosses the river mouth. This quantity is crucial for understanding wave-influenced delta morphodynamics, as it controls asymmetry, downdrift sediment availability, coastal sediment budget, and stratigraphic architecture. Quantifying β is essential for coastal management and predicting delta responses to human interventions and sediment supply changes. Here, β was computed as the ratio of the total LST_{Up} fraction arriving immediately downdrift the river mouth (LST_{Up_mouth}) to the total LST_{Up} entering the model domain.

$$\beta = \frac{\sum LST_{Up\_mouth}}{\sum LST_{Up}} \tag{3}$$

β is strongly correlated with Si_{Max} ($r^2 = 0.89$, Figure 2a), revealing that increasing wave dominance leads to increasing sediment bypassing across the river mouth. The relationship of β with Si computed with both LST_{Up} and LST_{MaxRM} is shown in Figures S4b and S4c in Supporting Information S1. With increasing wave dominance, β increases abruptly following a sigmoid relation with Si_{Max} (Figure 2a) around $Si_{Max} = 1$, when LST_{MaxRM} equals Qs. Values for β start to increase for $Si_{Max} > 0.5$ while complete bypassing occurs when Si_{Max} exceeds values around 1.5 to 2, corresponding to a doubling of LST_{MaxRM} relative to Q_s. Our results suggest that deltas with low values of β (<0.3) but displaying an Si value close to 1 can quickly switch to high β values with just a decrease of

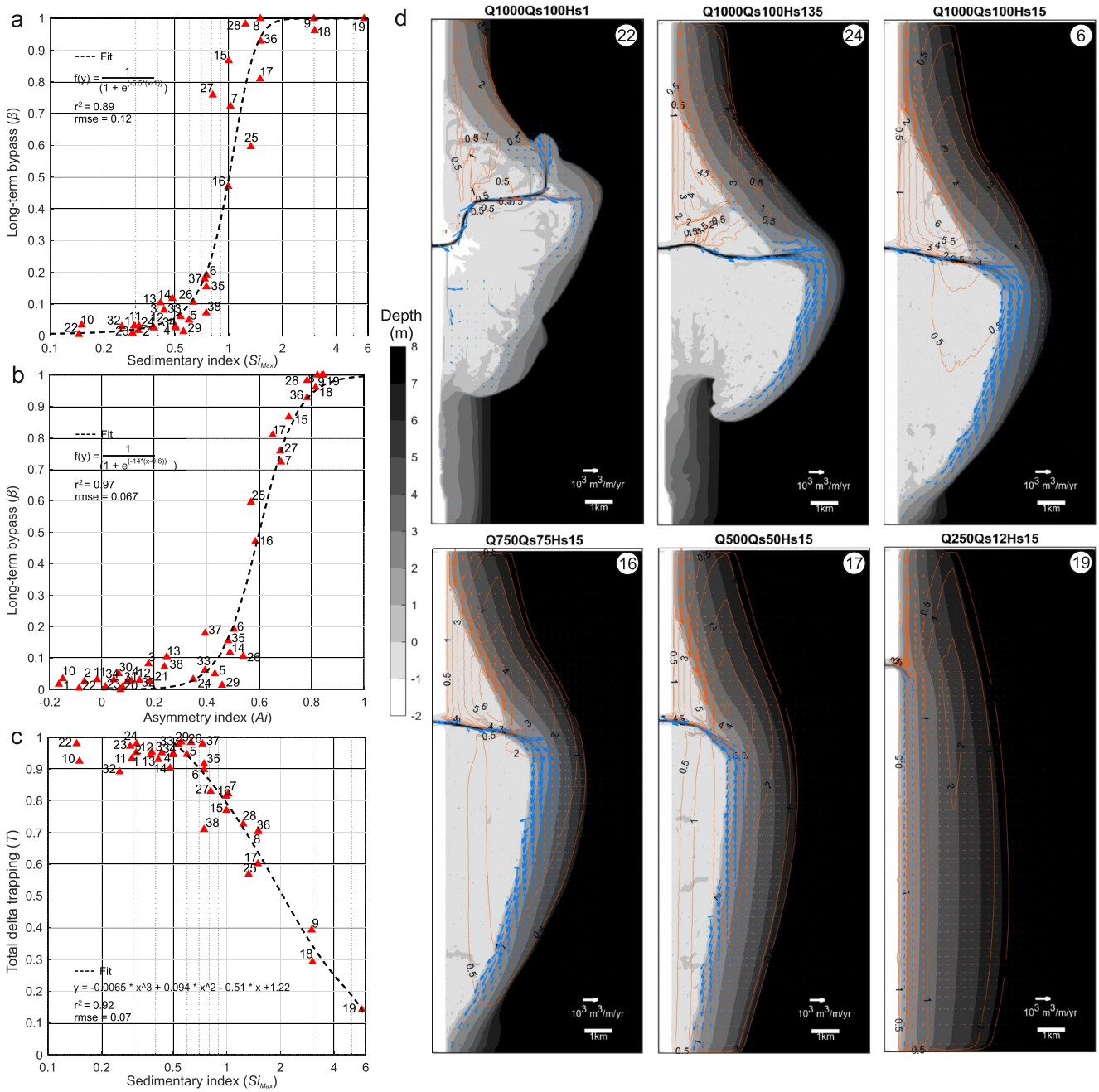

Figure 2. Long-term sediment bypass fraction (β) and total delta sediment trapping fraction (T) relates to the Sedimentary index (Si_{Max}). β forms a sigmoid function over Si_{Max} (a); β can be inferred from the Asymmetry index (Ai, b); T decreases with Si_{Max} (c). Examples of delta morphologies (d) expected for a range of Si_{Max}. Wave direction is from 45°. Updrift-sourced marine sand fraction is displayed with orange vectors and riverine sand fraction with blue vectors. Contours and numbers are the sand deposit thickness sourced from updrift (LST_{Up}).

40%–70% in sediment quantity (Figures 2a–2d). This bypass transition occurring when $Si \sim 1$, suggests that LST_{MaxRM} is a fundamental property in delta morphodynamics marking an inflection point in the system's behavior. Moreover, results also show that it is possible to infer β just from delta asymmetry ($r^2 = 0.97$; Figure 2b), a finding of importance for delta reconstructions. A delta lobe with high Ai indicates significant sediment bypass across the river mouth or preferential downdrift transport and deposition, resulting in downdrift lobe enlargement. Based on this relationship, we propose tentative β values for real-world deltas $\beta(Ai)$ (Table S2 in Supporting Information S1). Real-world deltas with $Ai < 0.4$ exhibit minimal sediment bypass ($\beta \approx 0$), while

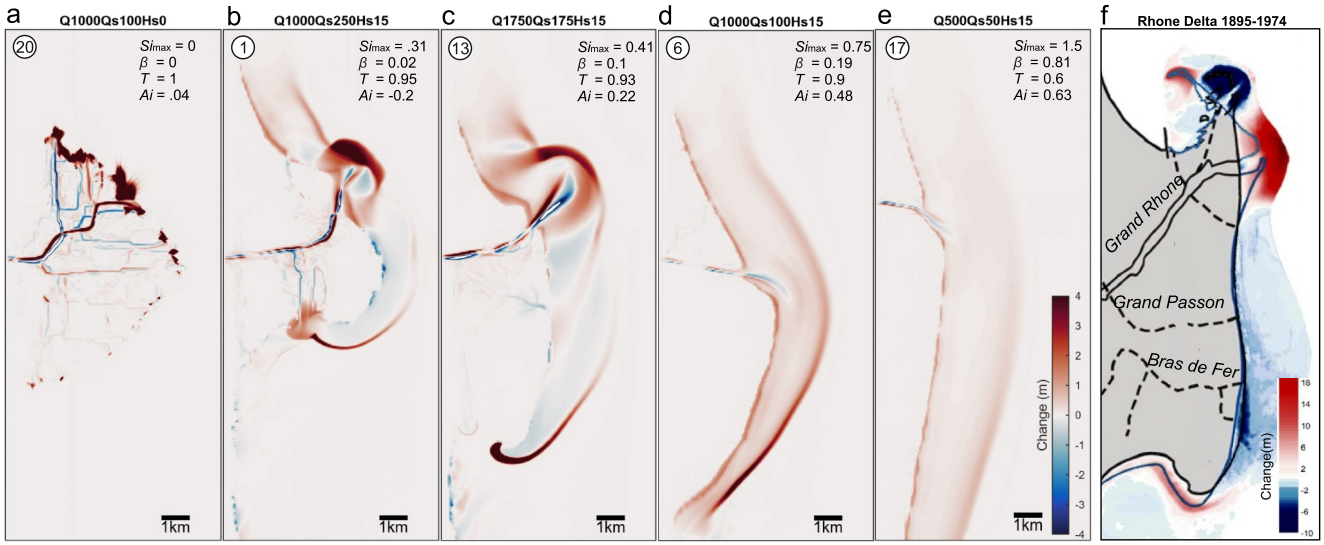

Figure 3. Subaqueous delta morphodynamics evidenced on the *Si* continuum shows transition from purely fluvial (a), to mixed (b, c), and to wave-dominated controls (d, e), decreasing avulsion timescale and increasing lobe diffusion. Comparison with the intermediate wave-influenced Rhone Delta (f, adapted from Sabatier et al., 2006) reveals similar avulsion styles and morphodynamics with mixed (hybrid) modeled systems: river mouth depocenters and mouth bars; sediment-starved shorefaces and the formation of spits downdrift.

those with $0.4 < Ai < 0.7$ likely experience low or episodic bypass and are highly susceptible to increased β following sediment reduction, whereas deltas with $Ai > 0.7$ consistently display high β values. The $\beta(Ai)$ values represent long-term averages of sediment bypass and do not account for modern behavior, which is influenced by changes in Qs due to dams. The correlation between Ai and Si_{Max} is consistent across both modeled data predictions of real-world deltas (Nienhuis et al., 2020; Figure S5 in Supporting Information S1), validating the relationship between delta asymmetry and bypass. Additionally, Si was tested against the river mouth balance metric (J) used to predict β at river mouths (Nienhuis, Ashton, Nardin, et al., 2016), but the latter offers no predictive capability for long-term bypass ($r^2 = 0$; Figure S4 in Supporting Information S1). The sediment fraction trapped in the delta plain (T) is the sum of sediment quantities entering the model domain (LST_{Up}, Qs) expressed as volume divided by the total volume of sediment captured in the model domain (V_{Sed}) at the end of each simulation.

$$T = \frac{\sum LST_{Up} + \sum Qs}{V_{Sed}} \tag{4}$$

When sediment removal exceeds deposition at the river mouth, deflected delta lobes and the loss of both longshore and riverine sources from the delta lobe system ensue (Figure 2c). In nature, remobilized sediment is often trapped in spit ends, or transported further downdrift, whereas in numerical cases remobilized sediment can leak out of the model domain. T indicates that leakage occurs as Si_{Max} approaches 0.5 to 1, whereas only a subaqueous delta forms at high Si (>5) (Figure 2). This type of behavior downdrift of the river mouth where only subaqueous deposition occurs has been documented for the contemporary morphodynamics of the Danube's Sf. Gheorghe lobe and the Brazos delta lobe following upstream reductions of sediment supply (Carlin & Dellapenna, 2015; Zăinescu et al., 2019), and for the highly wave-dominated Waipaoa system (Moriarty et al., 2015).

3.3. Transition of Delta Morphodynamics: From River to Wave Domination

The synthetic delta-lobes depict realistic salient mesoscale features like mouth bars, shorefaces, and spits across the wave dominance continuum, enabling in-depth analysis of shoreface morphodynamics (Figure 3). Symmetric mouth bars that orient into the direction of waves, similar to the Grand Rhone lobe (Figures S3a and S3b in Supporting Information S1) form with lesser wave domination, a situation where river mouths can orient into the prevailing direction of waves (Anthony, 2015). At higher wave domination, asymmetric mouth bars form at river mouth similar to the Sf. Gheorghe mouth of the Danube (Figures S3c and S3d in Supporting Information S1).

Numerical delta lobes with no wave influence show purely fluvial dynamics via localized avulsion-controlled depocenters at the delta front (Figure 3a). This autogenic signal arises even when all boundary conditions remain constant. As relative wave power increases, deltas initially transition into a hybrid state exhibiting both fluvial and wave-dominated characteristics with concurrent avulsion and wave redistribution processes (Figures 3b, 3c, and 3f). These delta lobes show localized river depocenters and extensive remobilization in the abandoned far reaches, leading to retreating shorelines and spits, a behavior that is reported for wave-influenced deltas such as the Rhone (Sabatier et al., 2006) and Godavari (Rao et al., 2015), and is well replicated by the model. The modern Chilia lobe (Danube) transitioned from a river-dominated bird-foot delta with multiple outlets in the late 19th century to a mixed wave-and-river influenced asymmetric morphology following net sediment reduction in the 1940 s (Preoteasa et al., 2021; Vespremeanu-Stroe et al., 2017). The model conceptually replicates the abandonment of updrift channels and the formation of downdrift depocenters (Figures 3b–3d).

Asymmetric wave climates tend to reduce river avulsion frequency because waves can effectively redistribute sediments along the shoreline (Hu et al., 2022). Delta lobes with higher wave domination ($Si > 0.5$), develop single river channels with a stable orientation and they exhibit downdrift asymmetry, reflected also in the subaqueous mouth bars. Sediment depocenters become increasingly elongated and diffuse due to wave redistribution, contributing to entire delta-front progradation commonly involving the formation of beach ridges, as in the lobes of the Danube (Sf. Gheorghe, Sulina; Vespremeanu-Stroe et al., 2016); and the Nile (Damietta, Rosetta; El-Asmar, 2000). Greater fluvial influence results in decreased Ai, and increased avulsion rates as seen in the Rhone. This behavior toward frequent avulsion versus stable behavior can also potentially be influenced by grain size and slope-induced effects (Caldwell & Edmonds, 2014; Edmonds & Slingerland, 2010; Orton & Reading, 1993).

3.4. Mechanism of Updrift LST (LST_{Up}) Trapping and Delta Plain Morphogenesis

Trapping of longshore-transported sediment in the updrift delta is instrumental in creating asymmetry in delta-lobe systems such as the Danube, Sao Francisco, Guadiana or Usumacinta-Grijalva and to the formation of extensive updrift beach-ridge plains (Dominguez, 2023; Nooren et al., 2017; Vespremeanu-Stroe et al., 2016). Lobe inception starts with the development of a downdrift skewed deltaic plain, until the shoreline orientation at the river mouth readjusts to the general direction of incoming waves (Figure 4a). When updrift sediment trapping occurs, the shoreline in the vicinity of the river mouth curves to reach an orientation normal to the angle of incoming waves. LST_{Up} decreases progressively along-coast and approaches zero even before directly interacting with the river jet or plume at the river mouth (orange arrows in Figure 4a). This signifies that large-scale shoreline orientation and mouth bar configuration, regulated by fluvial sediment supply at the river mouth, govern the interactions with LST. As illustrated by the simulations (Figures 4b and 4c), the largest beach ridge plains of a delta lobe are formed when the updrift coast is only slightly curved (concave), allowing for a long accretional coastal stretch to keep pace with the river-mouth advance over a long period. This observation corroborates the large-scale morphological blocking effect (Ashton & Giosan, 2011; Zăinescu et al., 2021) as a prevailing mechanism for updrift longshore transport trapping. The hydraulic "groin effect" (Giosan, 2007) immediately updrift of river mouths has been attributed to wave-current interactions and depth refraction, creating a localized zone of reduced updrift alongshore transport, which may hinder immediate sediment bypassing (Nienhuis, Ashton, Nardin, et al., 2016). However, this localized effect cannot fully explain the large-scale sediment trapping occurring over several kilometers updrift of river mouths (Figure 4), being more significant for updrift spit formation rather than for extensive beach ridge plain development. The updrift part of the simulated lobes contains LST_{Up}-derived sand bodies that reach their maximum relative volume when β is small (<0.2) and wave influence is moderate ($0.5 < Si < 1$) (Figure 4c). High Qs leads to a mixture of riverine and longshore sediment sources in the updrift part. This interplay between large-scale shoreline orientation, fluvial sediment supply, and wave-driven longshore transport suggests that large-scale morphological blocking primarily drives updrift sediment trapping in wave-influenced deltas.

4. Conclusions and Implications for Delta Vulnerability

This study leverages idealized Delft3D simulations to examine long-term evolution of deltaic lobe evolution under asymmetric, oblique waves. The synthetic deltas replicate well natural lobe asymmetry and highlight key dynamics of delta lobe systems, including stratigraphy, sediment bypass and trapping, governed by balances of riverine sediment supply and wave-driven longshore transport.

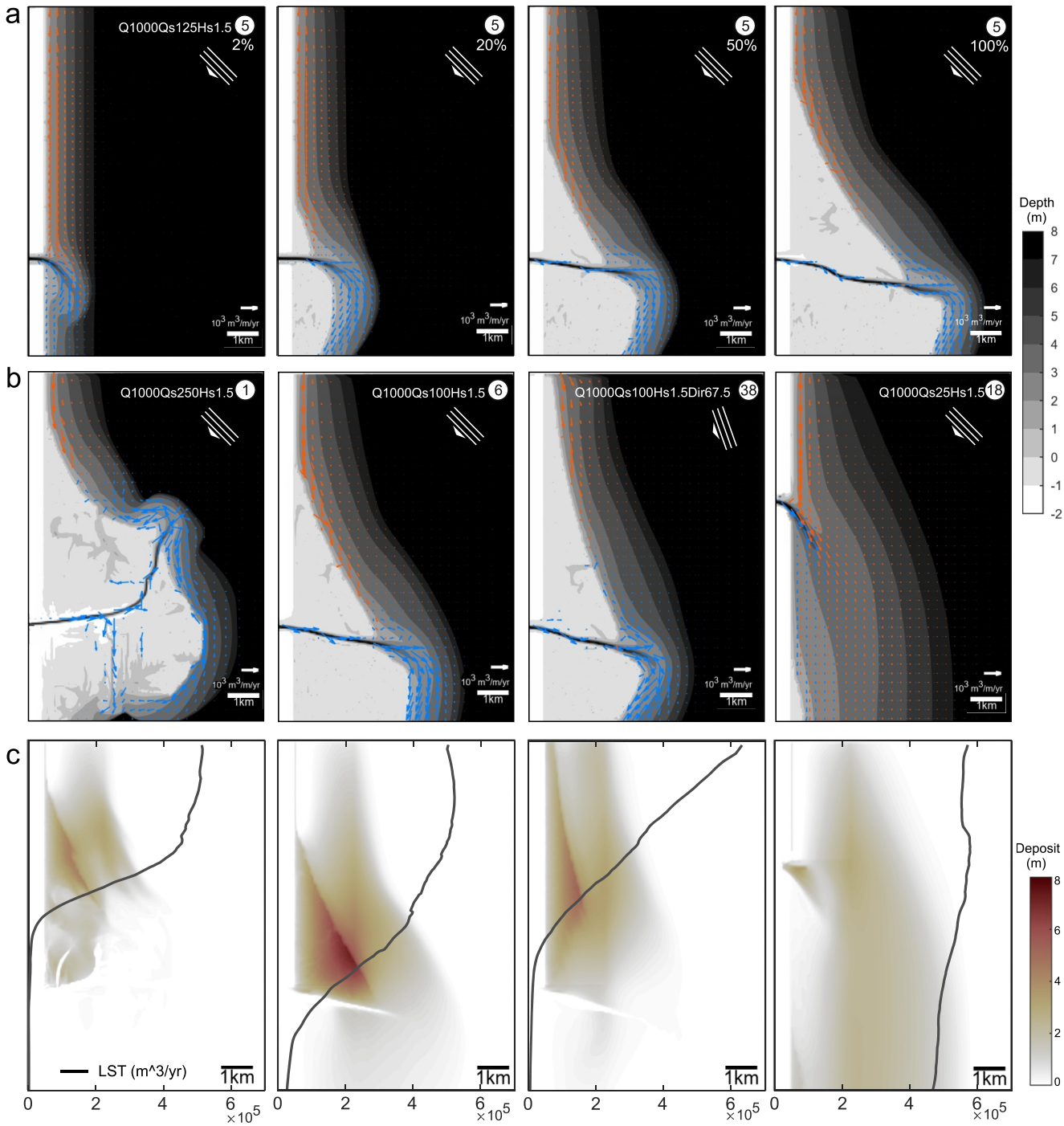

Figure 4. Longshore sediment trapping and beach ridge plain morphogenesis, showcasing both subaerial and subaqueous domains. Development of an updrift beach ridge plain for simulation #5 (Table S1 in Supporting Information S1) during different time intervals indicated by the percentage of the total duration (from 2% to 100%) (a). Orange vectors signify wave-driven LST_{Up} whereas the blue vectors are the riverine (Qs) sediment fraction. Final results showing beach ridge plain morphology of simulations #1, #6, #38, and #18 (b). Resultant thickness of the simulated sediment deposit and alongshore sediment transport rates (black line) of LST_{Up} (c) for simulations in panel (b).

Delta morphodynamics transitions from an avulsion-affected river-dominated style, characterized by shifting depocenters at river mouths, to a more stable, diffusive wave-dominated evolution style with single river channels and increased sediment bypass. Using the Sedimentary index (Si_{Max}) as an indicator of the degree of wave

domination of the delta lobe, we show that this transition occurs at $Si_{Max} > 0.5$. This dichotomy forms the basis for understanding hybrid, wave-influenced systems.

Delta lobes with mixed river-wave influences have a complex coastal dynamic wherein accumulating and retreating sectors alternate, driven by avulsions and river mouth sources, along with the diffusion of abandoned river mouths once upstream sediment supply is redirected. This type of behavior, exemplified by the Rhone delta and the Chilia lobe (Danube delta), poses a significant challenge for delta and coastal management (Sabatier et al., 2009).

Bypassing of longshore sediments across river mouths has significant implications for the morphological evolution of delta lobes. Critical changes occur when Si_{Max} approaches 1, indicating equal magnitudes of longshore sediment transport at the river mouth (LST_{MaxRM}) and fluvial sediment transport rates (Qs). Our data suggests an inflexion point around this value, where delta lobes exhibit increased asymmetry and sediment bypass fractions (β) rapidly transition from low (<~0.2) to near-complete bypass (~1) by a decrease of 40%–70% in Qs (Figure 2, Table S1 in Supporting Information S1). Lobes like Sf. Gheorghe (Danube) or Damietta (Nile) (Table S2 in Supporting Information S1) are highly vulnerable to anthropogenic sediment reduction. This may trigger rapid transitions from full updrift longshore sediment transport trapping to complete bypassing leading to erosion at river mouths and large-scale readjustments to a more deflected state. This is already an ongoing process at the Sf. Gheorghe mouth with sediment bypass likely switched from trapping at the beginning of 20th century to full bypass presently (Preoteasa et al., 2016; Zăinescu et al., 2019). Effective delta management in these systems must address reduced sediment supply which can significantly influence delta morphodynamics and sustainability. Wave dominated delta systems that trap less than 50% of the total fluvial sediment load ($T < 0.5$) at $Si_{Max} > 2$. While the simplified modeling in this study used a single sand grain size, real-world river mouths and deltas involve multiple sediment fractions of varying compaction, erodibility, and therefore transport potentials. Consequently, the practical application of simple sediment balances such as the Si to real-world individual deltas remains challenging given the sensitivity of β. Future research should focus on refining the accuracy of longshore sediment transport in real-world deltas, particularly at the river mouths where current predictions achieve order-of-magnitude accuracy (Nienhuis et al., 2015).

While predicting specific lobe evolution remains challenging, the systemic changes in similarly shaped lobes are more certain. It is useful to conceptualize the modeled synthetic delta lobes (Figures 1 and 2) as equilibrium morphological states toward which delta lobes gravitate following disturbances or changes in boundary conditions. However, adaptation timescales for real-world deltaic lobes will inherently be harder to predict exactly as they depend on the spatial scales of the lobe system, sediment cohesion properties, and the complex morphological feedbacks involved. Notably, even small changes in sediment quantities can significantly alter delta morphodynamics and long-term bypass rates. The inflexion point that occurs when riverine sediment deposition approaches wave-transported volumes can potentially shift long-term bypass rates from 0 to 1 with small changes in sediment quantities. This sensitivity underscores the importance of precise sediment transport quantification in understanding delta evolution under changing environmental conditions and human interventions.

Data Availability Statement

The Delft3D configuration files and data visualization and outputs across all simulations are accessible via our Zenodo repository (Zăinescu, Storms, Vespremeanu-Stroe, et al., 2023). Data processing and figure generation were performed using Matlab 2022b https://www.mathworks.com/. Delft3D 4 software can be downloaded from https://oss.deltares.nl/web/delft3d/downloads.

Acknowledgments
We thank Ningjie Hu, Brad Murray and two anonymous reviewers for their helpful comments. Center National d'Études Spatiales (CNES) is thanked for financing the postdoc project of FZ. Part of the research was supported by the Norway Grants 2014–2021 (project code RO-NO-2019-0415/contract no. 30/2020).

References

Aadland, T., & Helland-Hansen, W. (2019). Progradation rates measured at modern river outlets: A first-order constraint on the pace of deltaic deposition. *Journal of Geophysical Research: Earth Surface*, *124*(2), 347–364. https://doi.org/10.1029/2018JF004750

Aagaard, T., Anthony, E. J., Gillies, B., Laursen, S. N., Sukstorf, F. N., & Breuning-Madsen, H. (2021). Holocene development and coastal dynamics at the Keta Sand Spit, Volta River delta, Ghana. *Geomorphology*, *387*, 107766. https://doi.org/10.1016/j.geomorph.2021.107766

Anthony, E., Almar, R., & Aagaard, T. (2016). Recent shoreline changes in the Volta River delta, West Africa: The roles of natural processes and human impacts. *African Journal of Aquatic Science*, *41*(1), 81–87. https://doi.org/10.2989/16085914.2015.1115751

Anthony, E. J. (2015). Wave influence in the construction, shaping and destruction of river deltas: A review. *Marine Geology*, *361*, 53–78. https://doi.org/10.1016/j.margeo.2014.12.004

Anthony, E. J., & Blivi, A. B. (1999). Morphosedimentary evolution of a delta-sourced, drift-aligned sand barrier–lagoon complex, western Bight of Benin. *Marine Geology*, *158*(1–4), 161–176. https://doi.org/10.1016/S0025-3227(98)00170-4

Ashton, A. D., & Giosan, L. (2011). Wave-angle control of delta evolution. *Geophysical Research Letters*, *38*(13). https://doi.org/10.1029/2011GL047630

Attema, Y. (2014). *Delft3D model of the Ayeyarwady delta Myanmar* (p. 69). Deltares.

Bhattacharya, J. P., & Giosan, L. (2003). Wave-influenced deltas: Geomorphological implications for facies reconstruction. *Sedimentology*, *50*(1), 187–210. https://doi.org/10.1046/j.1365-3091.2003.00545.x

Broaddus, C. M., Vulis, L. M., Nienhuis, J. H., Tejedor, A., Brown, J., Foufoula-Georgiou, E., & Edmonds, D. A. (2022). First-order river delta morphology is explained by the sediment flux balance from rivers, waves, and tides. *Geophysical Research Letters*, *49*(22), e2022GL100355. https://doi.org/10.1029/2022GL100355

Caldwell, R. L., & Edmonds, D. A. (2014). The effects of sediment properties on deltaic processes and morphologies: A numerical modeling study. *Journal of Geophysical Research: Earth Surface*, *119*(5), 961–982. https://doi.org/10.1002/2013JF002965

Carlin, J. A., & Dellapenna, T. M. (2015). The evolution of a subaqueous delta in the Anthropocene: A stratigraphic investigation of the Brazos River delta, TX USA. *Continental Shelf Research*, *111*, 139–149. https://doi.org/10.1016/j.csr.2015.08.008

Dominguez, J. M. L. (2023). The wave-dominated deltas of Brazil. In J. M. L. Dominguez, R. K. P. de Kikuchi, M. C. de A. Filho, R. Schwamborn, & H. Vital (Eds.), *Tropical marine environments of Brazil: Spatio-temporal heterogeneities and responses to climate changes* (pp. 75–110). Springer International Publishing. https://doi.org/10.1007/978-3-031-21329-8_4

Edmonds, D. A., Chadwick, A. J., Lamb, M. P., Lorenzo-Trueba, J., Murray, A. B., Nardin, W., et al. (2021). Morphodynamic modeling of riverriver-dominated deltas: A review and future perspectives. In *Reference Module in Earth Systems and Environmental Sciences*. https://doi.org/10.1016/B978-0-12-818234-5.00076-6

Edmonds, D. A., & Slingerland, R. L. (2010). Significant effect of sediment cohesion on delta morphology. *Nature Geoscience*, *3*(2), 105–109. https://doi.org/10.1038/ngeo730

El-Asmar, H. M. (2000). Geoenvironmental changes along Gamasa-Baltim coast, north of the Nile Delta, Egypt. *Zeitschrift für Geomorphologie*, *44*(1), 59–73. https://doi.org/10.1127/zfg/44/2000/59

Gao, W., Nienhuis, J., Nardin, W., Wang, Z. B., Shao, D., Sun, T., & Cui, B. (2020). Wave controls on deltaic shoreline-channel morphodynamics: Insights from a coupled model. *Water Resources Research*, *56*(9). https://doi.org/10.1029/2020WR027298

Geleynse, N., Storms, J. E. A., Walstra, D.-J. R., Jagers, H. R. A., Wang, Z. B., & Stive, M. J. F. (2011). Controls on river delta formation; insights from numerical modelling. *Earth and Planetary Science Letters*, *302*(1–2), 217–226. https://doi.org/10.1016/j.epsl.2010.12.013

George, D. A., & Hill, P. S. (2008). Wave climate, sediment supply and the depth of the sand–mud transition: A global survey. *Marine Geology*, *254*(3–4), 121–128. https://doi.org/10.1016/j.margeo.2008.05.005

Giosan, L. (2007). Morphodynamic feedbacks on deltaic coasts: Lessons from the wave-dominated Danube Delta. *Coastal Sediments ', 07* (pp. 828–841). https://doi.org/10.1061/40926(239)63

Hori, K., Saito, Y., Zhao, Q., & Wang, P. (2002). Architecture and evolution of the tide-dominated Changjiang (Yangtze) River delta, China. *Sedimentary Geology*, *146*(3–4), 249–264. https://doi.org/10.1016/S0037-0738(01)00122-1

Hu, N., Murray, A. B., Ratliff, K. M., Little, Z., & Hutton, E. W. H. (2022). Wave-climate asymmetry influence on delta evolution and river dynamics. *Geophysical Research Letters*, *49*(9), e2021GL096315. https://doi.org/10.1029/2021GL096315

Jerolmack, D. J. (2009). Conceptual framework for assessing the response of delta channel networks to Holocene sea level rise. *Quaternary Science Reviews*, *28*(17–18), 1786–1800. https://doi.org/10.1016/j.quascirev.2009.02.015

Khan, S., Vincent, H., & Wilson, B. (2021). The late holocene erin deflected and asymmetric wave-dominated delta—Puerto Grande Bay, Trinidad. *Marine Geology*, *439*, 106545. https://doi.org/10.1016/j.margeo.2021.106545

Korus, J. T., & Fielding, C. R. (2015). Asymmetry in Holocene river deltas: Patterns, controls, and stratigraphic effects. *Earth-Science Reviews*, *150*, 219–242. https://doi.org/10.1016/j.earscirev.2015.07.013

Leonardi, N., Canestrelli, A., Sun, T., & Fagherazzi, S. (2013). Effect of tides on mouth bar morphology and hydrodynamics: Effect of Tides on Mouth Bar. *Journal of Geophysical Research: Oceans*, *118*(9), 4169–4183. https://doi.org/10.1002/jgrc.20302

Lesser, G. R., Roelvink, J. A., van Kester, J. A. T. M., & Stelling, G. S. (2004). Development and validation of a three-dimensional morphological model. *Coastal Engineering*, *51*(8–9), 883–915. https://doi.org/10.1016/j.coastaleng.2004.07.014

Moriarty, J. M., Harris, C. K., & Hadfield, M. G. (2015). Event-to-seasonal sediment dispersal on the Waipaoa River Shelf, New Zealand: A numerical modeling study. *Continental Shelf Research*, *110*, 108–123. https://doi.org/10.1016/j.csr.2015.10.005

Rao, K. N., Saito, Y., Nagakumar, K. C. V., Demudu, G., Rajawat, A. S., Kubo, S., & Li, Z. (2015). Palaeogeography and evolution of the Godavari delta, east coast of India during the Holocene: An example of wave-dominated and fan-delta settings. *Palaeogeography, Palaeoclimatology, Palaeoecology*, *440*, 213–233. https://doi.org/10.1016/j.palaeo.2015.09.006

Nardin, W., & Fagherazzi, S. (2012). The effect of wind waves on the development of river mouth bars. *Geophysical Research Letters*, *39*(12). https://doi.org/10.1029/2012GL051788

Nardin, W., Mariotti, G., Edmonds, D. A., Guercio, R., & Fagherazzi, S. (2013). Growth of river mouth bars in sheltered bays in the presence of frontal waves. *Journal of Geophysical Research: Earth Surface*, *118*(2), 872–886. https://doi.org/10.1002/jgrf.20057

Nienhuis, J. H., Ashton, A. D., Edmonds, D. A., Hoitink, A. J. F., Kettner, A. J., Rowland, J. C., & Törnqvist, T. E. (2020). Global-scale human impact on delta morphology has led to net land area gain. *Nature*, *577*(7791), 514–518. https://doi.org/10.1038/s41586-019-1905-9

Nienhuis, J. H., Ashton, A. D., & Giosan, L. (2015). What makes a delta wave-dominated? *Geology*, *43*(6), 511–514. https://doi.org/10.1130/G36518.1

Nienhuis, J. H., Ashton, A. D., & Giosan, L. (2016). Littoral steering of deltaic channels. *Earth and Planetary Science Letters*, *453*, 204–214. https://doi.org/10.1016/j.epsl.2016.08.018

Nienhuis, J. H., Ashton, A. D., Nardin, W., Fagherazzi, S., & Giosan, L. (2016). Alongshore sediment bypassing as a control on river mouth morphodynamics. *Journal of Geophysical Research: Earth Surface*, *121*(4), 664–683. https://doi.org/10.1002/2015JF003780

Nooren, K., Hoek, W. Z., Winkels, T., Huizinga, A., Van Der Plicht, H., Van Dam, R. L., et al. (2017). The Usumacinta–Grijalva beach-ridge plain in southern Mexico: A high-resolution archive of river discharge and precipitation. *Earth Surface Dynamics*, *5*(3), 529–556. https://doi.org/10.5194/esurf-5-529-201

Orton, G. J., & Reading, H. G. (1993). Variability of deltaic processes in terms of sediment supply, with particular emphasis on grain size. *Sedimentology*, *40*(3), 475–512. https://doi.org/10.1111/j.1365-3091.1993.tb01347.x

Preoteasa, L., Vespremeanu-Stroe, A., Dan, A., Ţuţuianu, L., Panaiotu, C., Stoica, M., et al. (2021). Late-Holocene landscape evolution and human presence in the northern Danube delta (Chilia distributary lobes). *The Holocene*, *31*(9), 1459–1475. https://doi.org/10.1177/09596836211019121

Preoteasa, L., Vespremeanu-Stroe, A., Tătui, F., Zăinescu, F., Timar-Gabor, A., & Cîrdan, I. (2016). The evolution of an asymmetric deltaic lobe (Sf. Gheorghe, Danube) in association with cyclic development of the river-mouth bar: Long-term pattern and present adaptations to human-induced sediment depletion. *Geomorphology*, *253*, 59–73. https://doi.org/10.1016/j.geomorph.2015.09.023

Ratliff, K. M., Hutton, E. H. W., & Murray, A. B. (2018). Exploring wave and sea-level rise effects on delta morphodynamics with a coupled river-ocean model. *Journal of Geophysical Research: Earth Surface*, *123*(11), 2887–2900. https://doi.org/10.1029/2018JF004757

Robinet, A., Idier, D., Castelle, B., & Marieu, V. (2018). A reduced-complexity shoreline change model combining longshore and cross-shore processes: The LX-Shore model. *Environmental Modelling and Software*, *109*, 1–16. https://doi.org/10.1016/j.envsoft.2018.08.010

Sabatier, F., Maillet, G., Provansal, M., Fleury, T.-J., Suanez, S., & Vella, C. (2006). Sediment budget of the Rhône delta shoreface since the middle of the 19th century. *Marine Geology*, *234*(1–4), 143–157. https://doi.org/10.1016/j.margeo.2006.09.022

Sabatier, F., Samat, O., Ullmann, A., & Suanez, S. (2009). Connecting large-scale coastal behaviour with coastal management of the Rhône delta. *Geomorphology*, *107*(1–2), 79–89. https://doi.org/10.1016/j.geomorph.2006.09.026

Sadio, M., Anthony, E., Diaw, A., Dussouillez, P., Fleury, J., Kane, A., et al. (2017). Shoreline changes on the wave-influenced Senegal River Delta, West Africa: The roles of natural processes and human interventions. *Water*, *9*(5), 357. https://doi.org/10.3390/w9050357

Storms, J., Stive, M., Roelvink, D. J. A., & Walstra, D.-J. (2007). Initial morphologic and stratigraphic delta evolution related to Buoyant River Plumes. *Coastal Sediments '07*, 736–748. https://doi.org/10.1061/40926(239)56

Su, M., Yao, P., Wang, Z. B., Zhang, C. K., & Stive, M. J. F. (2017). Exploratory morphodynamic hindcast of the evolution of the abandoned Yellow River delta, 1578–1855 CE. *Marine Geology*, *383*, 99–119. https://doi.org/10.1016/j.margeo.2016.11.007

Syvitski, J., Anthony, E., Saito, Y., Zăinescu, F., Day, J., Bhattacharya, J. P., & Giosan, L. (2022). Large deltas, small deltas: Toward a more rigorous understanding of coastal marine deltas. *Global and Planetary Change*, *218*, 103958. https://doi.org/10.1016/j.gloplacha.2022.103958

Syvitski, J., & Saito, Y. (2007). Morphodynamics of deltas under the influence of humans. *Global and Planetary Change*, *57*(3–4), 261–282. https://doi.org/10.1016/j.gloplacha.2006.12.001

van der Vegt, H., Storms, J. E. A., Walstra, D.-J. R., Nordahl, K., Howes, N. C., & Martinius, A. W. (2020). Grain size fractionation by process-driven sorting in sandy to muddy deltas. *The Depositional Record*, *6*(1), 217–235. https://doi.org/10.1002/dep2.85

Vespremeanu-Stroe, A., Preoteasa, L., Zăinescu, F., Rotaru, S., Croitoru, L., & Timar-Gabor, A. (2016). Formation of Danube delta beach ridge plains and signatures in morphology. *Quaternary International*, *415*, 268–285. https://doi.org/10.1016/j.quaint.2015.12.060

Vespremeanu-Stroe, A., Zăinescu, F., Preoteasa, L., Tătui, F., Rotaru, S., Morhange, C., et al. (2017). Holocene evolution of the Danube delta: An integral reconstruction and a revised chronology. *Marine Geology*, *388*, 38–61. https://doi.org/10.1016/j.margeo.2017.04.002

Walsh, J. P., & Nittrouer, C. A. (2009). Understanding fine-grained river-sediment dispersal on continental margins. *Marine Geology*, *263*(1–4), 34–45. https://doi.org/10.1016/j.margeo.2009.03.016

Wright, L. D., & Coleman, J. M. (1972). River delta morphology: Wave climate and the role of the subaqueous profile. *Science*, *176*(4032), 282–284. https://doi.org/10.1126/science.176.4032.282

Wright, L. D., & Coleman, J. M. (1973). Variations in morphology of major river deltas as functions of ocean wave and river discharge regimes. *AAPG Bulletin*, *57*. https://doi.org/10.1306/819A4274-16C5-11D7-8645000102C1865D

Zăinescu, F., Anthony, E., & Vespremeanu-Stroe, A. (2021). River jets versus wave-driven longshore currents at river mouths. *Frontiers in Marine Science*, *8*. https://doi.org/10.3389/fmars.2021.708258

Zăinescu, F., Storms, J. E. A., van der Vegt, H., Schuster, M., Vespremeanu-Stroe, A., & Anthony, E. (2023). Field-informed modeling of complex asymmetric wave influenced delta lobes. In *Coastal sediments '23*.

Zăinescu, F., Storms, J. E. A., Vespremeanu-Stroe, A., van Der Vegt, H., Schuster, M., & Anthony, E. (2023). Wave-influenced delta morphodynamics, long-term sediment bypass and trapping controlled by relative magnitudes of riverine and wave-driven sediment transport (Version 1) [Dataset]. *Zenodo*. https://doi.org/10.5281/zenodo.13472805

Zăinescu, F., Vespremeanu-Stroe, A., Anthony, E., Tătui, F., Preoteasa, L., & Mateescu, R. (2019). Flood deposition and storm removal of sediments in front of a deltaic wave-influenced river mouth. *Marine Geology*, *417*, 106015. https://doi.org/10.1016/j.margeo.2019.106015

References From the Supporting Information

Baar, A. W., Boechat Albernaz, M., van Dijk, W. M., & Kleinhans, M. G. (2019). Critical dependence of morphodynamic models of fluvial and tidal systems on empirical downslope sediment transport. *Nature Communications*, *10*(1), 4903. https://doi.org/10.1038/s41467-019-12753-x

Battjes, J. A., & Janssen, J. P. F. M. (1978). Energy loss and set-up due to breaking random waves. *Coastal Engineering Proceedings*, *16*, 32. https://doi.org/10.9753/icce.v16.32

Cohen, S., Kettner, A. J., Syvitski, J. P. M., & Fekete, B. M. (2013). WBMsed, a distributed global scale riverine sediment flux model: Model description and validation. *Computers & Geosciences*, *53*, 80–93. https://doi.org/10.1016/j.cageo.2011.08.011

Dan, S., Walstra, D.-J. R., Stive, M. J. F., & Panin, N. (2011). Processes controlling the development of a river mouth spit. *Marine Geology*, *280*(1–4), 116–129. https://doi.org/10.1016/j.margeo.2010.12.005

Dean, R. G. (1991). Equilibrium beach profiles: Characteristics and applications. *Journal of Coastal Research*, *7*(1), 53–84.

Deltares. (2010). *Delft3D-FLOW user manual* (p. 694). Deltares.

Dominguez, J. M. L., & Guimarães, J. K. (2021). Effects of Holocene climate changes and anthropogenic river regulation in the development of a wave-dominated delta: The São Francisco River (eastern Brazil). *Marine Geology*, *435*, 106456. https://doi.org/10.1016/j.margeo.2021.106456

Isobe, M., & Horikawa, K. (1982). Study on water particle velocities of shoaling and breaking waves. *Coastal Engineering in Japan*, *25*(1), 109–123. https://doi.org/10.1080/05785634.1982.11924340

Komar, P. D. (1998). *Beach processes and sedimentation* (p. 544). Prentice Hall.

Komen, G. J., Hasselmann, K., & Hasselmann, K. (1984). On the existence of a fully developed wind-sea spectrum. *Journal of Physical Oceanography*, *14*(8), 1271–1285. https://doi.org/10.1175/1520-0485(1984)014<1271:OTEOAF>2.0.CO;2

Lenstra, K. J. H., Ridderinkhof, W., & Vegt, M. (2019). Unraveling the mechanisms that cause cyclic channel-shoal dynamics of ebb-tidal deltas: A numerical modeling study. *Journal of Geophysical Research: Earth Surface*, *124*(12), 2778–2797. https://doi.org/10.1029/2019JF005090

Nardin, W., & Fagherazzi, S. (2018). The role of waves, shelf slope, and sediment characteristics on the development of erosional chenier plains. *Geophysical Research Letters*, *45*(16), 8435–8444. https://doi.org/10.1029/2018GL078694

Roelvink, D., & Reniers, A. (2011). A guide to modeling coastal morphology. *World Scientific*, *12*. https://doi.org/10.1142/7712

Roelvink, J. A., & Walstra, D. J. (2004). Keeping it simple by using complex models. *Advances in Hydro-science and Engineering*, *6*, 1–11.

Sánchez-Arcilla, A., & Jiménez, J. A. (1997). A morphological "Mixed-Type" model for the Ebro Delta Coast. *Coastal Engineering*, *1996*, 2806–2819. https://doi.org/10.1061/9780784402429.217

Shore Protection Manual. (1984). CERC, waterways experiment station (Vicksburg, USA).

Trombetta, T. B., Marques, W. C., Guimarães, R. C., & Costi, J. (2020). An overview of longshore sediment transport on the Brazilian coast. *Regional Studies in Marine Science*, *35*, 101099. https://doi.org/10.1016/j.rsma.2020.101099

van der Wegen, M., & Roelvink, J. A. (2012). Reproduction of estuarine bathymetry by means of a process-based model: Western Scheldt case study, The Netherlands. *Geomorphology*, *179*, 152–167. https://doi.org/10.1016/j.geomorph.2012.08.007

van Rijn, L. C., & Walstra, D. J. R. (2004). Description of TRANSPOR2004 and Implementation in Delft3D-ONLINE. 66.

Van Rijn, L. C. (2006). *Principles of sedimentation and erosion engineering in rivers, Estuaries and coastal seas*. Aqua Publications. Retrieved from www.aquapublications.nl

van Rijn, L. C. (2007). Unified view of sediment transport by currents and waves. II: Suspended transport. *Journal of Hydraulic Engineering*, *133*(6), 668–689. https://doi.org/10.1061/(ASCE)0733-9429(2007)133:6(668)

Van Rijn, L. C. (2014). A simple general expression for longshore transport of sand, gravel and shingle. *Coastal Engineering*, *90*, 23–39. https://doi.org/10.1016/j.coastaleng.2014.04.008

Zăinescu, F. I., Vespremeanu-Stroe, A., & Tătui, F. (2019). The formation and closure of the Big Breach of Sacalin spit associated with extreme shoreline retreat and shoreface erosion. *Earth Surface Processes and Landforms*, *44*(11), 2268–2284. https://doi.org/10.1002/esp.4639